Climatology and Meteorological Evolution of Major Wildfire Events over the Northeast United States

JOSEPH B. POLLINA* AND BRIAN A. COLLE

School of Marine and Atmospheric Sciences, Stony Brook University, Stony Brook, New York

JOSEPH J. CHARNEY

USDA Forest Service, East Lansing, Michigan

(Manuscript received 26 January 2012, in final form 31 July 2012)

ABSTRACT

This study presents a spatial and temporal climatology of major wildfire events, defined as >100 acres burned (>40.47 ha, where 1 ha = 2.47 acre), in the northeast United States from 1999 to 2009 and the meteorological conditions associated with these events. The northeast United States is divided into two regions: region 1 is centered over the higher terrain of the northeast United States and region 2 is primarily over the coastal plain. About 59% of all wildfire events in these two regions occur in April and May, with ~76% in region 1 and ~53% in region 2. There is large interannual variability in wildfire frequency, with some years having 4–5 times more fire events than other years. The synoptic flow patterns associated with northeast United States wildfires are classified using the North American Regional Reanalysis. The most common synoptic pattern for region 1 is a surface high pressure system centered over the northern Appalachians, which occurred in approximately 46% of all events. For region 2, the prehigh anticyclone type extending from southeast Canada and the Great Lakes to the northeast United States is the most common pattern, occurring in about 46% of all events. A trajectory analysis highlights the influence of large-scale subsidence and decreasing relative humidity during the events, with the prehigh pattern showing the strongest subsidence and downslope drying in the lee of the Appalachians.

1. Introduction

a. Motivation

Wildfires are an important forecast problem with significant societal impacts. Across the United States, ~4.7 million (~500 000) acres burn on average each year from wildfires west (east) of the Mississippi River (NIFC 2008). [This is equivalent to ~1.9 million (~202 430) ha, where 1 ha = 2.47 acre.] Wildfires in the northeast United States (Fig. 1) have resulted in 13 633 acres burned on average annually, which is 0.27% of the total acres burned within the contiguous United States (NIFC 2008).

Although large wildfires are relatively rare in the northeast United States (NEUS), they can still have substantial impacts. For example, the ''Sunrise Fire'' in late August 1995 burned ~7000 acres across portions of the Pine Barrens region of eastern Long Island, New York (Hamilton and Ostapow 2009), destroying or damaging several homes, businesses, and five fire trucks. On 17 April 2008, the ''Overlooks'' wildfire burned over 3000 acres in Minnewaska State Park Preserve near New Paltz, New York. The spread of the fire was aided by unusually dry surface meteorological conditions relative to the NEUS [20%–25% relative humidity (RH)]. Forest rangers were forced to close all roads in the 20 000-acre park, and the fire was not contained until 22 April 2008 (Buckley 2008). It was the largest fire in the park in the last 60 years.

b. Fire weather forecasting

When preparing a fire weather forecast, a forecaster must consider the meteorological ingredients that impact wildfire potential in the planetary boundary layer

* Current affiliation: NOAA/National Weather Service Forecast Office, Upton, New York.

Corresponding author address: Dr. Brian A. Colle, School of Marine and Atmospheric Sciences, Stony Brook University, Stony Brook, NY 11794-5000.
E-mail: brian.colle@stonybrook.edu

DOI: 10.1175/WAF-D-12-00009.1

© 2013 American Meteorological Society

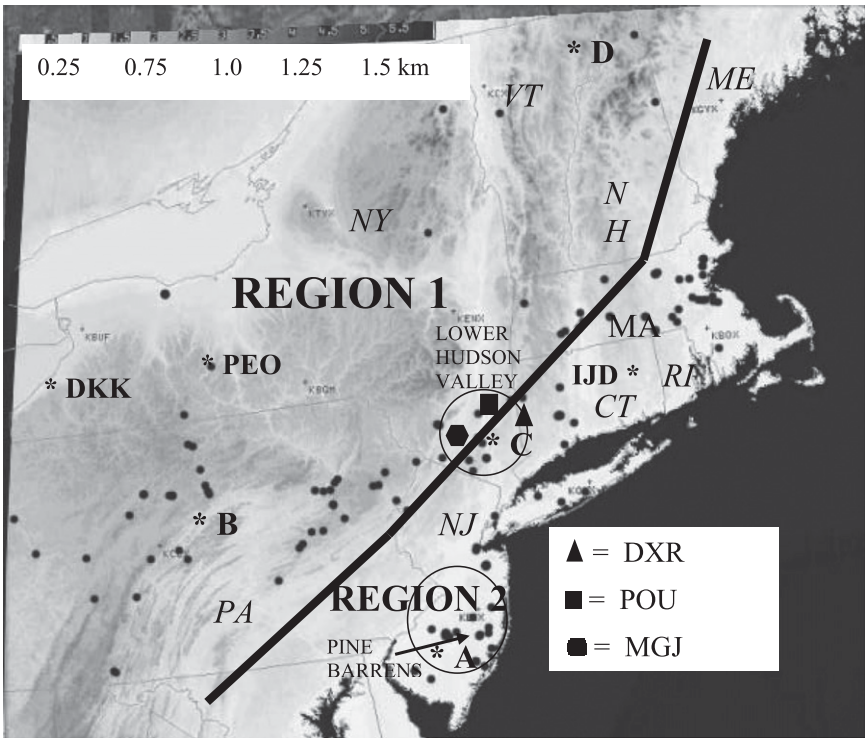

FIG. 1. Topographical map (shaded, km) of the NEUS and the two regions used in this study separated by the thick black line. The dots represent locations of major fires (>100 acres) from 1999 to 2009. The boldface asterisks are the starting points of the backward trajectories, where A = 1, B = 2, C = 3, and D = 4, as well as the stations used in Fig. 17, and the surface stations used in Fig. 15 are given by the three-letter identifier.

(PBL), such as wind speed and direction, RH, near-surface temperature, precipitation, and atmospheric stability. One must also account for the potential influence of topography and available surface fuels for wildfire ignition and behavior. Low-level winds determine the rate and direction of fire spread (Bureau of Meteorology 2009). The moisture content of the fuels tends to decrease as the surface temperature increases and the RH decreases, thus increasing the potential for a wildfire (Bureau of Meteorology 2009; Kassomenos 2010). In addition, higher air temperature increases the probability that fuels will reach their ignition temperature. Atmospheric stability affects the development of the fire plume, which in turn affects the potential for high-momentum and dry air aloft to mix downward into the fire environment (Charney and Keyser 2010).

An important component of the National Weather Service (NWS) effort to protect life and property is the anticipation of wildfire threat days, which are days exhibiting elevated potential for the ignition and spread of wildfires. There are two common methods for assessing wildfire threat and communicating the threat to the general public. The first method is the National Fire Danger Rating System (NFDRS; Burgan 1988). The NFDRS uses topographical data, meteorological data from Remote Automated Weather Stations, and fuel conditions to generate a wildfire threat assessment, which includes the ratings of low, moderate, high, very high, and extreme. It is used by the fire community to anticipate the potential for wildfires to occur and ensure that necessary resources are available to fight wildfires (Burgan 1988).

The second method of assessing and communicating wildfire threat is the issuance of fire weather watches (FWWs) or red flag warnings (RFWs). The NWS issues FWWs or RFWs for an area when certain predefined meteorological criteria favoring wildfire development are met. The criteria are locally defined for a particular forecast area. For example, at the New York City, New York, NWS Forecast Office, an FWW or RFW is issued in the spring and fall when sustained surface winds or gusts exceed 11.2 m s^{-1} (21.7 kt), RH is <30%, and the rainfall during the last 3 days is <0.64 cm (<0.25 in.). In the summer, the criteria is the same except rainfall during the last 5 days must be <0.64 cm, and the Keetch–Byram drought index (Keetch and Byram 1968) must be above 300 (NWS 2008). An FWW is issued

24–72 h prior to an event when the probability of exceeding the above thresholds is 30%–70%, while an RFW is issued within 24 h of an event if the probability is >70%. The probability is determined by a forecaster using all available data, including numerical weather prediction models, ensembles, and model output statistics.

Several studies have explored the meteorological ingredients that influence wildfire threat over the NEUS. In many cases, wildfires occur under high pressure and associated subsidence drying (Schaefer 1957). For some events the descent of strong winds and dry air from the middle troposphere to the PBL can enhance the potential for a fire to spread. For example, the Double Trouble State Park fire in central New Jersey occurred in the late afternoon on 2 June 2002 immediately following the passage of a dry and gusty cold front. Kaplan et al. (2008) and Charney and Keyser (2010) noted the importance of an intrusion of dry air from 550 to 750 hPa behind the front in facilitating the spread of the wildfire, which was mixed to the surface within the deep convective PBL to create drying behind the front.

c. *Fire weather synoptic patterns*

Several studies have related synoptic atmospheric patterns to wildfire occurrence over the NEUS. Schroeder et al. (1964) categorized the synoptic flows for critical fire weather ingredients across the lower 48 U.S. states from 1951 to 1960. They showed that high fire threat days in the NEUS can be associated with four types of pressure systems: Canadian high, Pacific high, Bermuda high, and Atlantic storm. If the high passes to the north of the Northeast region, high fire danger usually occurs after the passage of a cold front. If the high passes to the south, high fire danger usually occurs before the passage of a cold front on the western or northern side of the high. If there is a westward extension of the Bermuda high into the southern United States, the westerly flow limits the amount of low-level moisture from the Gulf of Mexico, which increases the fire danger.

Takle et al. (1994) used a synoptic weather classification system developed by Yarnal (1993) (Table 1) to highlight the different types of surface high and low pressure patterns associated with actual wildfire events in West Virginia. Of the several different Yarnal types of surface pressure patterns, Takle et al. (1994) found that the western side of a departing high pressure system was the most common pattern for wildfires in West Virginia. Also, a surface high pressure region centered to the south contributes to drying conditions in West Virginia due to westerly downslope flow in the lee of the Appalachians. One goal of the current study is to extend the Yarnal classification to the remainder of the NEUS.

TABLE 1. Modified Yarnal synoptic classification scheme.

Yarnal classification	Description
Extended high (EH)	Covers a large area, sometimes with multiple centers
Prehigh (PH)	High building in after the passage of the cold front; centered to the west or northwest of the northeast United States
Back of high (BH)	Western side of high pressure system; high is usually centered off the east coast
High to the south (HS)	Center of high pressure to the south, with low pressure to the north; leads to westerly winds
High to the north (HN)	Center of high pressure to the north, with low pressure to the south; leads to easterly winds
Elongated low (EL)	An elongated area of low pressure, covering a relatively large area, sometimes with multiple centers
Cyclonic with rain (RC)	Area is under cyclonic flow with rain
Cold front (CF)	Cold front moving through
Surface trough (ST)	An region of relatively low atmospheric pressure at the surface that is not associated with a cold front or warm front

The Yarnal classification system will be discussed in more detail in section 2.

d. *Research questions*

While there have been some case studies investigating fire weather events over the NEUS (e.g., Charney and Keyser 2010; Kaplan et al. 2008), no known extensive fire weather climatologies have been published for this region. Schroeder et al. (1964) presented an analysis of the synoptic types for NEUS. wildfires, but they only concentrated on ''critical fire weather'' days instead of actual wildfires, and included a limited number of synoptic patterns in their analysis. Given the impact that wildfires can have on life and property, especially in the densely populated NEUS, it is important to better understand the ambient conditions that increase the likelihood of wildfire ignition and spread in this area. A fire weather climatology will help forecasters recognize the features that are associated with the increased risk of NEUS wildfires. In particular, this research will address the following questions:

- How does wildfire occurrence vary monthly and interannually over the NEUS?
- What are the most common synoptic weather patterns associated with wildfires in the NEUS?
- What is the origin of dry air near the top of the PBL associated with many NEUS wildfire events?

TABLE 2. The year, month, and day of the actual fires in region 1. Those dates with an asterisk indicate that a fire also occurred in region 2 on that date.

29 Apr 1999	11 Apr 2002	16 Apr 2003*	6 May 2005	30 Apr 2006	7 May 2007
31 Jul 1999	18 Apr 2002	20 May 2003	7 May 2005	1 May 2006*	17 Apr 2008
14 Apr 1999*	11 May 2002	19 Apr 2004	11 May 2005	2 May 2006	19 Apr 2008
29 Apr 2001*	8 Jul 2002	14 Nov 2004	1 Oct 2005	3 May 2006	24 Mar 2009
3 May 2001*	2 Aug 2002	9 Apr 2005	30 Mar 2006	5 May 2006	18 Apr 2009*
30 Oct 2001	11 Aug 2002	16 Apr 2005	20 Apr 2006	6 May 2006	25 Apr 2009
1 Mar 2002	15 Apr 2003	17 Apr 2005	29 Apr 2006	10 May 2006	26 Apr 2009

2. Data and methods

Fire weather climatology over the NEUS

The fire weather climatology from January 1999 through December 2009 over the NEUS was constructed by first identifying actual wildfire days, defined for this study as days on which one or more major (>100 acres burned) wildfires occurred in the NEUS (Fig. 1). Wildfire occurrence data were obtained through the Northeast Interagency Coordination Center (NICC) and the Pennsylvania Bureau of Forestry, and 155 major wildfires were identified. Since topography, population, and land surface characteristics are key factors for wildfires, the NEUS was divided into two subregions. Region 1 includes much of the higher elevations of the NEUS (Fig. 1), while region 2 is located in the lee of the Appalachians and includes most of the coastal plain and the largest urban areas. When identifying the actual wildfire days, a day on which multiple fires occurred in a region was only counted once. Wildfires occurred on 42 days in region 1 (Table 2) and on 73 days in region 2 (Table 3), and on some days wildfires occurred in both regions. Average monthly surface temperatures and precipitation totals for the NEUS were obtained from the National Climatic Data Center (NOAA 2011) to compute temperature and precipitation anomalies for those years that experienced a relatively large number of major fires.

A modified Yarnal (1993) synoptic classification system was used to determine the large-scale surface pressure patterns associated with the actual wildfire days (Table 1). The eight different types of surface pressure patterns identified by Yarnal were used, and an additional ninth category associated with a surface trough was added for this study. Figure 2 shows examples of five of the Yarnal synoptic types used for this NEUS study. The ''prehigh'' synoptic type occurs when surface high pressure builds southeastward over the NEUS (Fig. 2a), which typically occurs after the passage of a cold front. The surface high centered to the northwest of the NEUS contributes to northwesterly flow over the region. For the ''extended high'' (Fig. 2b), the center of surface high pressure is directly over the NEUS, with light winds across the region. The ''back of high'' pattern has the center of the high located just to the east of the East Coast (Fig. 2c), which allows for southwesterly flow over the NEUS region. With ''high to the south'' (Fig. 2d), there is also typically a corresponding area of lower pressure to the north, with surface westerly flow between the two pressure centers. On the other hand, a high to the north and a corresponding low to the south allow for easterly flow across the NEUS (Fig. 2e). The other synoptic patterns from the Yarnal classification that are not shown are the elongated low, cyclonic with rain, cold front, and surface trough, which is a pressure trough that is not associated with a cold or warm front.

The National Centers for Environmental Prediction (NCEP) surface synoptic weather maps for 1200 UTC available from the University of Washington (http://www.atmos.washington.edu/data/vmaproom/varchive.cgi) were manually inspected to determine the Yarnal classification of each actual fire case in the dataset. If

TABLE 3. As in Table 2, but for region 2. Those dates with an asterisk indicate that a fire also occurred in region 1.

31 Mar 1999	8 Apr 2000	29 Apr 2004	21 Oct 2008
1 Apr 1999	3 Nov 2000	12 May 2004	21 Mar 2009
6 Apr 1999	25 Apr 2001	18 Apr 2004	17 Apr 2009
8 Apr 1999	28 Apr 2001	20 Apr 2005	18 Apr 2009*
14 Apr 1999*	29 Apr 2001*	12 May 2005	
24 Apr 1999	30 Apr 2000	26 Sep 2005	
27 Apr 1999	3 May 2001*	27 Jan 2006	
30 Apr 1999	4 May 2001	21 Mar 2006	
2 May 1999	10 Jun 2001	27 Mar 2006	
31 May 1999	26 Oct 2001	1 May 2006*	
6 Jun 1999	27 Oct 2001	8 May 2006	
8 Jun 1999	12 Nov 2001	9 May 2006	
19 Jun 1999	18 Nov 2001	19 Dec 2006	
8 Jul 1999	27 Apr 2002	8 May 2007	
15 Jul 1999	28 Apr 2002	9 May 2007	
18 Jul 1999	10 May 2002	15 May 2007	
26 Jul 1999	2 Jun 2002	3 Aug 2007	
3 Aug 1999	10 Jun 2002	17 Apr 2008*	
4 Aug 1999	15 Aug 2002	19 Apr 2008*	
6 Nov 1999	16 Apr 2003*	20 Apr 2008	
7 Nov 1999	18 May 2003	28 Apr 2008	
10 Nov 1999	16 Nov 2003	13 Jul 2008	
26 Mar 2006	24 Apr 2004	24 Aug 2008	

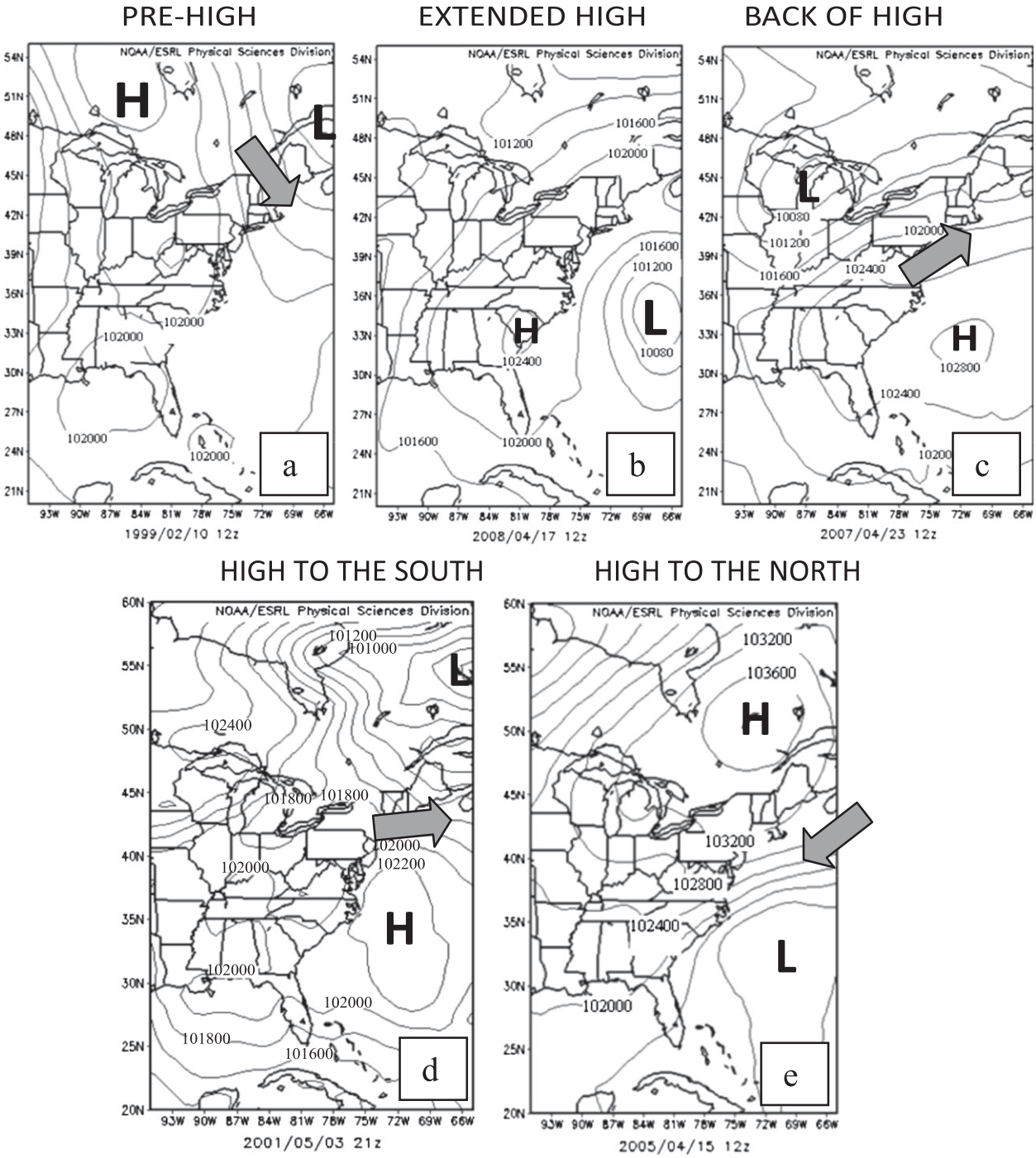

FIG. 2. Surface map examples of the Yarnal synoptic classification scheme showing sea level pressure every 4 hPa for (a) PH, (b) BH, (c) EH, (d) HS, and (e) HN. The surface wind direction is given by the shaded arrow.

there were missing images from the University of Washington web site, analyses from other web sites such as the Storm Prediction Center (http://www.spc.noaa.gov/obswx/maps/), Hydrometeorological Prediction Center (http://www.hpc.ncep.noaa.gov/html/sfc_archive.shtml), and Plymouth State University (http://vortex.plymouth.edu/u-make.html) were used.

The North American Regional Reanalysis (NARR; Mesinger et al. 2006) at 32-km horizontal grid spacing was used to composite the large-scale flow evolution and

other meteorological variables. Spatial composites were created for regions 1 and 2 separately using the actual fires dates. Since wildfire start times were not available for many fires, daily composites of sea level pressure (SLP) and 500-hPa geopotential heights were created on the date the fire was first reported. Since RH and low-level winds vary diurnally, the 2100 UTC [1700 eastern daylight time (EDT)] data from the NARR were used to composite the 2-m RH and 925-hPa winds, since this is typically closer to the warmest and driest time of day at 1800 UTC (1400 EDT).

The Hybrid Single-Particle Lagrangian Integrated Trajectory (HYSPLIT) model (Draxler and Rolph 2012; Rolph 2012) was used to determine the origin of the air near the top of the PBL (~850 hPa). Using the NARR reanalysis field, HYSPLIT computes three-dimensional parcel trajectories, which are available every 6 h (Mesinger et al. 2006). Backward trajectories at the surface were calculated for 48 h prior to the wildfire date starting at 2100 UTC.

3. Results

a. Major wildfire climatology

Humans are the main cause of wildfires over the NEUS, with approximately 81% of all events in the northeast United States resulting from human activity (Northeast States Emergency Consortium 2012). Lightning accounts for a much smaller fraction of wildfire starts in the NEUS (~7%) compared to the western United States, where dry thunderstorms and lightning are more common and responsible for many of the wildfires in that region (Rorig and Ferguson 2002).

Figure 1 shows the spatial distribution of the 155 major wildfires from 1999 to 2009 across regions 1 and 2 of the NEUS. About 61% (96 out of 155) of the wildfires occur in region 2 (~0.37 fires per 1000 km^2), while 39% occur in region 1 (~0.20 fires per 1000 km^2). Fires are clustered in Massachusetts, portions of southwest Connecticut, the lower Hudson Valley in New York, the Pine Barrens of southern New Jersey, and in central and northeastern Pennsylvania.

Figure 3 shows the annual number and percentage of major wildfires from 1999 to 2009 for regions 1 and 2. In region 1, the percentage was largest in 2006, which accounted for 10 of the 42 (~24%) fires in the time period. The 10 fires in region 1 for 2006 occurred in spring (March–May), with 6 fires occurring in May (not shown). Both 2002 and 2005 were also relatively active years in region 1, with seven fires in 2002 (four in the spring and three in summer) and eight fires in 2005 (six occurring in April and May). In contrast, the percentage of fires in region 2 peaks in 1999, with 22 out of 73 (~30%) occurring that year, and 10 of these 22 wildfires occurring in spring (7 in April).

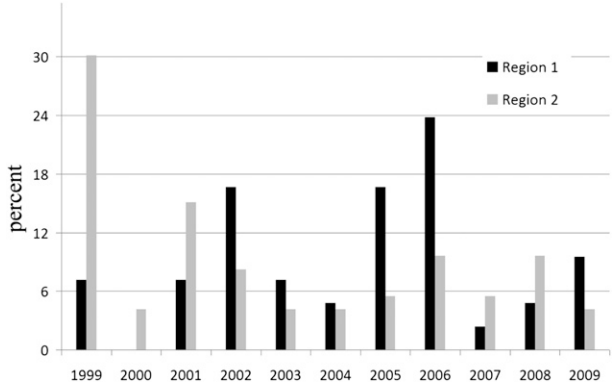

FIG. 3. Annual climatology of NEUS wildfire events for region 1 (black) and region 2 (gray) from 1999 to 2009.

Average monthly surface temperatures for the full NEUS showed that region 1 had warmer than normal daily average temperatures (by ~0.8°C) for those seasons with a high number of major fires (spring 2002, summer 2002, spring 2005, and spring 2006). Of the individual months during these seasons, only one of the warm season months (May 2005) was cooler than normal (by 2.4°C); however, there are not enough months in this sample to establish the statistical significance of this anomaly at the 90% level. For region 1, two of the four seasons that had a relatively high fire frequency were wetter than normal (spring 2002 and spring 2005), while the other two were drier than normal, suggesting that some active fire seasons are not anomalously dry.

For region 2, spring and summer temperatures in 1999 were above average by 0.7° and 1.0°C, respectively, and the July 1999 temperature was also above average by 1.6°C. Meanwhile, precipitation was 88% and 75% of normal for spring and summer of 1999, respectively. Note, however, that some fuel types in the NEUS will support a fire even after a recent precipitation event, if temperatures are sufficiently warm that surface fuels can dry out. Rothermel (1983) and Viney (1991) show that fuels that are less than 0.64 cm in diameter are most important in the start and spread of NEUS wildfires, since these fuels have small surface area and can dry quickly. Also, smaller areas of anomalously dry conditions within the larger NEUS region can contribute to fires on days that exhibit moist anomalies for the region as a whole.

The monthly distribution of major wildfire events was also determined for the two regions (Fig. 4). April and May together account for ~76% and ~53% of the fires in regions 1 and 2, respectively, with April alone having

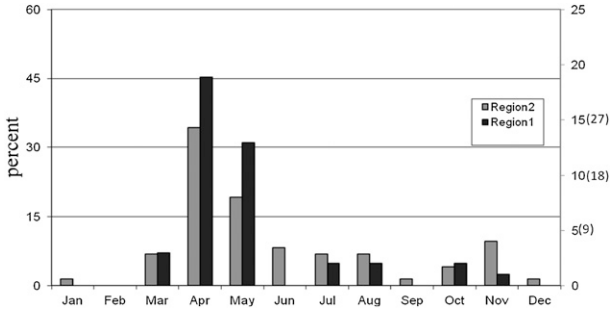

FIG. 4. Monthly climatology of NEUS wildfires for region 1 (black) and region 2 (gray). The left axis is the percentage of fires that occurred in a particular month and the right axis is the number of fires for region 1 (no parentheses) and region 2 (in parentheses).

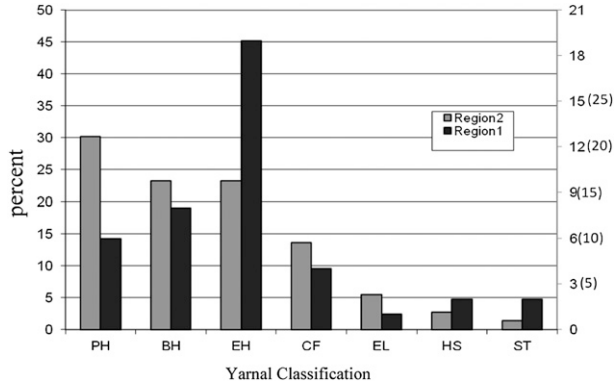

FIG. 5. A breakdown of wildfires over the NEUS in terms of the different Yarnal synoptic patterns in Table 1. The left axis is the percentage of fires that occurred for a particular synoptic type and the right axis is the number of fires for region 1 (no parentheses) and region 2 (in parentheses).

~45% in region 1 and ~34% in region 2. During early to midspring, vegetation across the NEUS has not experienced leaf-out, so dead leaves and twigs on the forest floor can rapidly dry out as the solar radiation and temperature increase during the early spring (Bureau of Meteorology 2009; Kassomenos 2010). In contrast, summer (June–August, JJA) accounts for only ~10% of the major wildfires in region 1 and ~22% in region 2 (Fig. 4). In summer, the vegetation typically holds abundant moisture, which prevents the fuels from igniting easily, and the relatively humid conditions are also less favorable for wildfires. During the winter (December–February, DJF) there is little or no wildfire activity (~0% for region 1 and ~3% for region 2), since the ground is cool, damp, and often snow covered. Also, since humans are the leading cause of wildfires in the NEUS, less outdoor human activity during the winter also favors fewer wildfires. As spring approaches and humans spend more time outdoors, there is an increased risk of wildfire activity.

b. Synoptic flow classification climatology

Figure 5 shows the climatology of synoptic flow patterns (defined in Table 1) for the actual wildfire days using the Yarnal classification scheme. The combination of prehigh (PH), back of high (BH), and extended high (EH) types account for ~78% of the wildfire events in region 1 and ~77% in region 2. The EH is the most common synoptic type in region 1 (~45% of all events), while the PH type is most common in region 2 (~30% of all cases). The combination of cold fronts (CF), elongated low (EL), high to the south (HS), surface trough (ST), and high to the north (HN) together account for ~21% and 23% of the fire events for regions 1 and 2, respectively. A CF is often accompanied by precipitation, so a relatively low percentage of major wildfires occur in this flow pattern (~10% of all cases in region 1 and 14% region 2). The EL type is also often associated with precipitation, and thus there were only a few fires in both regions for this flow regime. Meanwhile, the HN had no events in regions 1 and 2, since easterly flow advects cool and moist marine air from the Atlantic Ocean over the NEUS.

A bootstrap method (Zwiers 1990) was applied to the synoptic-type flow patterns to test for statistical significance. A new sample of the same size was generated 1000 times by randomly choosing from the original sample. The 95% confidence interval around the mean was determined by finding the 2.5th and 97.5th percentiles of the means of the 1000 samples. For region 1, the most common type (EH) was found to be statistically significant (95% level) compared to the other types, while PH, BH, and CF were not. For region 2, the more common types (PH, EH, and BH) were statistically significant, while CF was not.

Figure 6 shows the monthly percentage of actual fire days for each synoptic type in regions 1 and 2. For region 1 (Fig. 6a), during April the EH type occurs more than twice as often as the next most common synoptic type (CF), and more often than all the other types combined during May. EH and BH are the synoptic types most often associated with major wildfires in July and August in region 1. For region 2 (Fig. 6b), although the PH type is the most common pattern overall (~27%), it is not the most common type in any individual month. Rather, during the peak fire season (April) the PH occurs about as often as BH (~10%). Major wildfires in region 2 associated with CFs are most common in April, but also occur in May, June, July, and October.

Overall, the EH type is more common in region 1 (45% of all wildfire days) than region 2 (23% of all wildfire days), especially during the peak of fire season. About 45% of EHs were multiday (2 days or more) events (not shown). This allows for an extended period

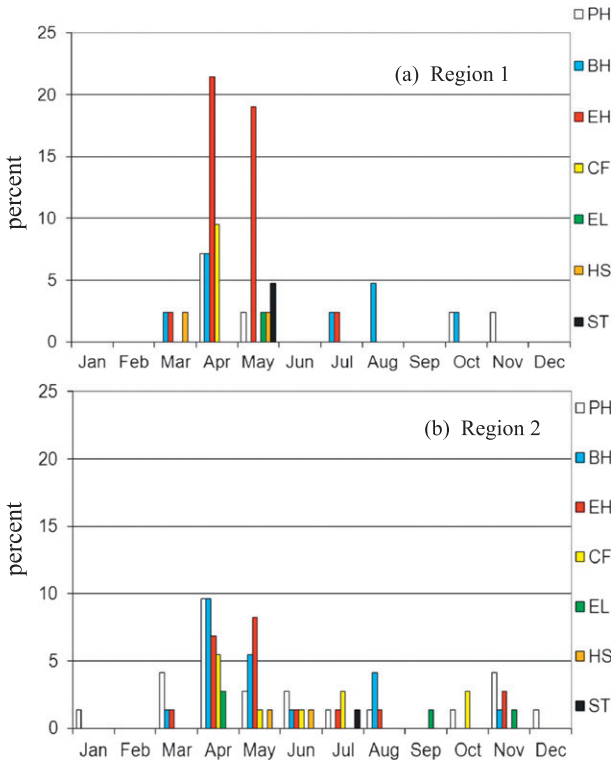

FIG. 6. A monthly climatology of the Yarnal synoptic types (listed in Table 1) for the NEUS wildfires in regions (a) 1 and (b) 2.

of drying and warming over the higher terrain of the NEUS (region 1). Wildfires may be less common for EH events in region 2 due to inland warming and low wind speeds, which allows the relatively cool and moist sea breeze to develop over coastal sections (Novak and Colle 2006), thus decreasing the wildfire risk.

c. *Synoptic composites*

As described in section 2, spatial composites were created using the NARR for the actual wildfire days in regions 1 and 2 separately. At 48 h prior ($t - 48$ h) to a fire event in region 1 (Fig. 7a), there is surface high pressure centered near the eastern Great Lakes and a weak surface low over the western Atlantic. The 925-hPa flow is 5 m s^{-1} or less over the NEUS, ranging from weak westerly and northwesterly over southern and western sections of the NEUS to more northerly over the remainder of the NEUS. The surface potential temperatures are 280–285 K over eastern New England, which is 2–4 K cooler than western portions of the NEUS. Meanwhile, a broad ridge at 500 hPa extends from the western Great Lakes south-southwestward to Texas (Fig. 7c). To the east of this ridge, the 500-hPa winds over the NEUS are northwesterly at ~10 m s^{-1}. The NEUS is situated between two wind maxima at 300 hPa (Fig. 7c): one maximum (20–25 m s^{-1}) located east of the NEUS coast and oriented southwest to northeast and the other (20–24 m s^{-1}) north of the Great Lakes in southern Canada. The northern part of the NEUS is in a favorable area for subsidence beneath the right jet-exit region (Fig. 7c).

On the day of the event ($t = 0$) in region 1 (Fig. 7b), the surface high is over Virginia, while the surface low off the mid-Atlantic coast is weaker than at $t - 48$ h. The 925-hPa flow over the northern NEUS is generally northwesterly, while light and variable winds exist over much of region 1 as the axis of the high pressure was located over the NEUS. Meanwhile, the low pressure area was east of the mid-Atlantic coast, which is similar to the EH pattern in the Yarnal classification (Fig. 2b). Potential temperatures are 2–3 K higher over northern and eastern portions of the NEUS than at $t - 48$ h. At 500 hPa (Fig. 7d), the ridge axis is over the central and eastern Great Lakes and has higher amplitude than at $t - 48$ h. The 500-hPa winds over the NEUS are northwesterly at about 10 m s^{-1}, with a wind maximum at 300 hPa (~28 m s^{-1}) to the north of the central Great Lakes region. The $t = 0$ composite analysis suggests that the NEUS is located in a favorable area for subsidence downstream of the upper-level ridge (Fig. 7d). The $t = 0$ composite analysis of 600–300-hPa vertical velocity indicates subsidence over the entire NEUS (Fig. 8a), with stronger downward vertical velocities occurring over central New York and northern Vermont and New Hampshire. To diagnose the large-scale vertical motion at mid- to upper levels, the forcing term from the Sutcliffe–Trenberth form of the quasigeostrophic omega equation (Trenberth 1978) was evaluated by calculating the advection of geostrophic relative vorticity by the thermal wind [Eq. (5.7.42) in Bluestein (1992)] in the 600–300-hPa layer. Using the composite analysis at $t = 0$, there is descent over much of the NEUS (Fig. 8b) in the 600–300-hPa layer, where there is negative advection of anticyclonic relative vorticity by the thermal wind in this layer.

Figure 9a shows the composite 2-m RH, 925-hPa wind, and 2-m temperature analyses over the NEUS for region 1 at $t - 48$ h. The lowest RHs (45%–55%) and warmest surface temperatures (16°–18°C) are mainly along the coastal plain from southeast Pennsylvania northeastward to Massachusetts. The RH is 15%–20% less than the daily climatology for the NARR across the NEUS, which is significant at the 95% level; however, the daily temperature is only 1°–2°C warmer than climatology and not statistically significant at the 90% level. Some of this warming and drying was likely from the 3–5 m s^{-1} northwesterly (downslope) flow off the Appalachians at 925 hPa at this time. At $t = 0$ in region 1

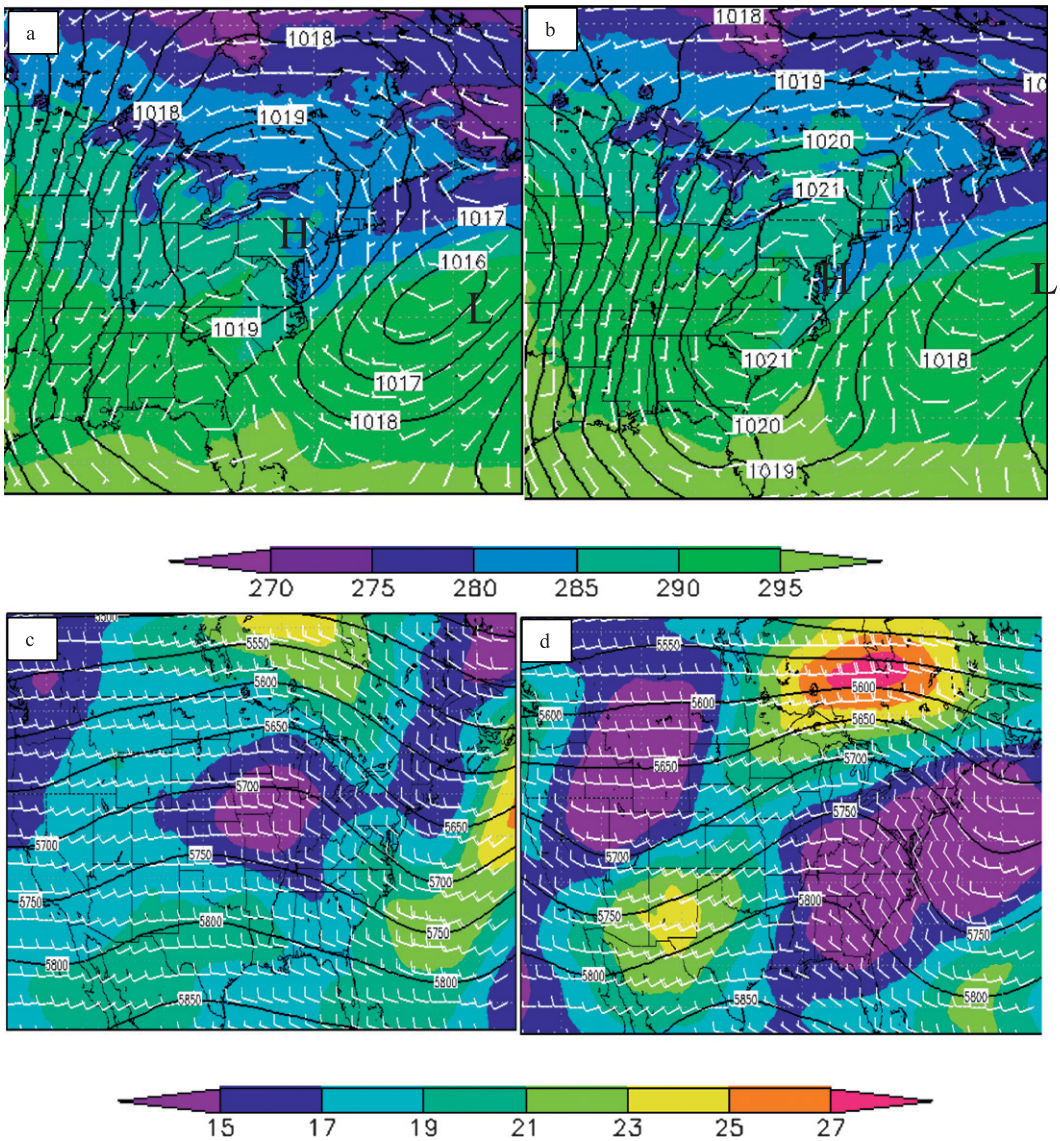

FIG. 7. Spatial composite of mean sea level pressure (MSLP; solid, every 1 hPa), 2-m potential temperature (color shaded, every 5 K), and winds (full barb = 10 m s^{-1}) at 925 hPa for (a) 48 h prior to a wildfire event in region 1 and (b) the day of the event. Composite 500-hPa heights (solid, every 30 m) and wind barbs (half barb = 5 m s^{-1}; full barb = 10 m s^{-1}), as well as 300-hPa wind speed (shaded, every 2 m s^{-1}), are shown for region 1 (c) 48 h prior to a wildfire event and (d) the day of the event ($t = 0$).

(Fig. 9b), the RHs generally are less than 50% across most of New Jersey and the eastern half of Pennsylvania. The 2-m temperatures are generally 2°–3°C warmer than at $t - 48$ h, with the warmest air over southeast Pennsylvania (20°–21°C), where westerly flow over high terrain in central Pennsylvania continues to favor downslope warming and drying. This composite analysis suggests that these fire events can occur when the RH values are greater and wind speeds are less than the criteria for a RFW (30% RH and 11.2 m s^{-1} wind speed); however, there is a positive surface moisture bias in the NARR that will be quantified below. There are also 5%–10% RH dry anomalies compared to climatology that exist at the surface 3–5 days before the event in the NARR, which is significant at the 90% level, while the temperature anomalies are only <1°C and not significant. This suggests that there can be a longer period of persistent drying before these events, and that surface RH anomalies may be more important than the temperature anomalies.

Figure 10a shows a cross section of potential temperature, horizontal winds, and vertical velocity along

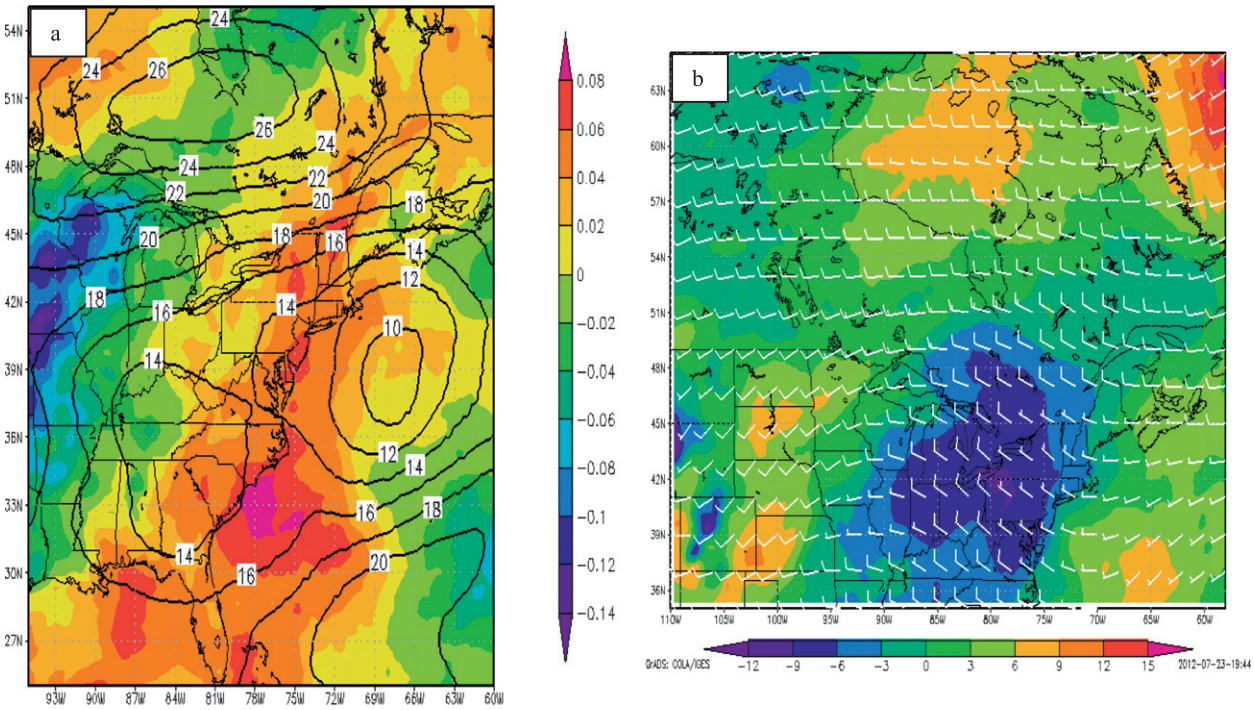

FIG. 8. (a) Composite of 600–300-hPa vertical velocity (color shaded, every 2 Pa s^{-1}) and 300-hPa wind speeds (solid, every 2 m s^{-1}) for the region 1 wildfire events on the day of the fire ($t = 0$), and (b) a composite of 600–300-hPa advection of absolute vorticity by the thermal wind (shaded, 10^{-12} Pa m^{-2} s^{-1}) from the Sutcliffe–Trenberth form of the QG omega equation (shaded, 10^{-12} Pa m^{-2} s^{-1}, with negative values showing downward motion forcing) from 600–300-hPa for region 1 wildfires.

latitude 41.5°N for the region 1 composite at $t - 48$ h. There is upward motion in the lower levels from near the surface to ~800 hPa between 80° and 75°W (region 1) in response to upslope westerly flow. Meanwhile, there is downward motion from 800 to 200 hPa, consistent with large-scale descent to the east of the midlevel ridge. The descending air extends downward to near the surface over western portions of region 2 as a result of downslope flow in the lee of the Appalachians. At $t = 0$ (Fig. 10b), region 1 generally exhibits upward motion from the surface to 800 hPa, with descending air at low levels limited to the east of 75°W. Figure 10a,b illustrate that both low-level downslope flow and dynamically driven subsidence over a deep layer are important for wildfires over much of the NEUS.

For the region 2 composite at $t - 48$ h (Fig. 11), there is a broad 500-hPa ridge over the central portions of the United States (Fig. 11c), while an upper-level trough extends ~750 km to the east of the east coast. The 500-hPa winds are northwesterly over the NEUS at 10–15 m s^{-1}, and there is a 300-hPa wind maximum (~22 m s^{-1}) oriented east to west from south-central Canada and the northern Great Plains to southeastern Canada. Meanwhile, surface high pressure is centered near western North Carolina and eastern Tennessee (Fig. 11a). A surface trough is located to the east over the western Atlantic. This trough most likely represents a cold front offshore, which is commonly associated with a PH synoptic type (Yarnal 1993). The 925-hPa winds are generally northwesterly at ~5 m s^{-1} or less, and potential temperatures range from 285–290 K in Pennsylvania and southern New England to 275–280 K over extreme northern NEUS. The trough offshore, along with a northwesterly flow, makes this similar to a PH-type pattern.

At $t = 0$ in region 2 (Fig. 11b), the PH-type pattern remains established across the NEUS, with the surface high pressure (~1020 hPa) over the Carolinas and westerly or west-northwesterly flow at 925 hPa. Wind speeds are ~5 m s^{-1} over the NEUS, with potential temperatures similar to those seen at $t - 48$ h (Fig. 11a). The 500-hPa pattern is similar at $t = 0$ (Fig. 11d), except that the ridge is more amplified over the northern plains, and the northwesterly winds to the east of the ridge have increased to ~25 m s^{-1}. At 300 hPa, there is a jet streak (~27 m s^{-1}) over southeastern Canada oriented northwest to southeast. As with region 1, there is subsidence over much of the NEUS from 600 to 300 hPa (Fig. 12a). The strongest sinking aloft is over northern New England, which is in a favored region for descent in the right

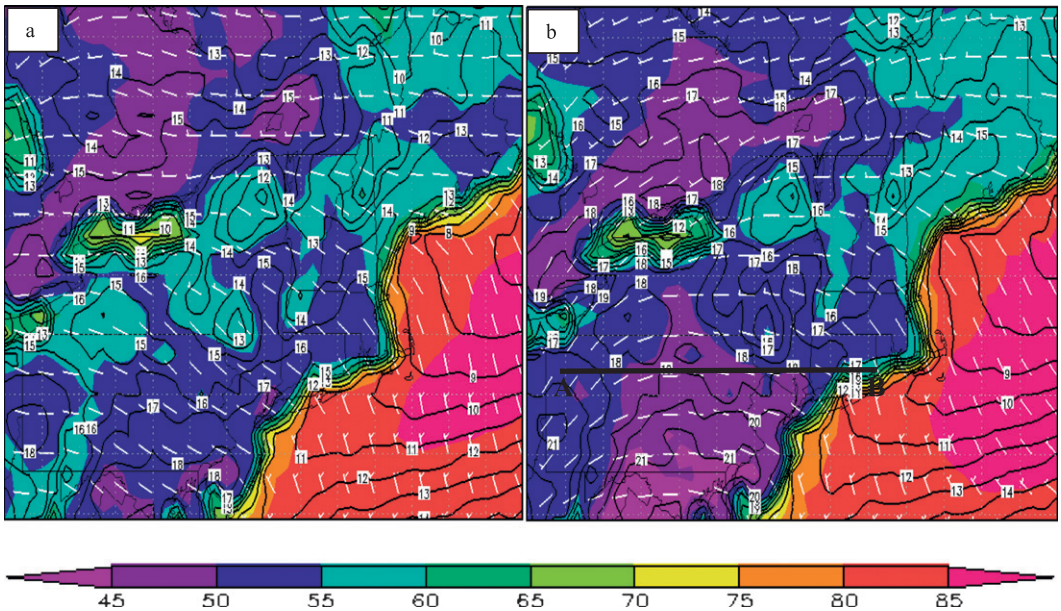

FIG. 9. Composite 2-m RH (color shaded, every 5%), 2-m temperature (solid, every 2°C), and 925-hPa winds (full barb = 10 m s^{-1}) for (a) 48 h prior and (b) day of (t = 0) the region 1 wildfire events. The location for cross section AB in Fig. 10 is shown by the thick black line in (b).

jet-exit region. The Sutcliffe–Trenberth analysis indicates forcing for descent over much of the NEUS at 600–300 hPa (Fig. 12b).

For region 2, at $t - 48$ h the lowest surface RHs (45%–50%) are to the east of the Appalachians (Fig. 13a), which is a 15%–25% dry anomaly compared to climatology in the NARR. As in region 1, there is also a 5%–10% dry anomaly 3–5 days before the event on average. At $t - 48$ h, the west-northwesterly winds favor downslope drying over the coastal plain, with low-level subsidence from the surface to about 700 hPa primarily to the east of 74.5°W at $t - 48$ h (Fig. 14a), and from the surface to about 500 hPa (Fig. 14b) east of 74.5°W at $t = 0$ (Fig. 14a), while more synoptic-scale subsidence exists from above these levels to 200 hPa (Figs. 14a,b). The terrain-forced subsidence (0.09 and 0.12 Pa s^{-1}) in the lee increases from $t - 48$ h to $t = 0$ (Figs. 14a,b), which corresponds with a 2°–3°C increase in surface temperature along the coastal NEUS but little change in NARR RH (Fig. 13b).

A comparison between NARR and actual surface observations for a few cases indicates that the NARR was too moist. Therefore, the average temperature and RH were calculated for each of the six stations in Fig. 1 at 2100 UTC (1700 EDT) using all wildfire events in the region where the station was located (Fig. 15). Most stations have an average surface temperature of ~20°C, which is within ~2°C of the composite NARR 2-m temperature for each region (cf. Fig. 9). In contrast, the average RH at the stations is 30%–40%, which is 20%–25% less than the NARR composite. Overall, this illustrates the difficulty in obtaining accurate low-level moisture analyses for these relatively dry fire events.

Since EH and PH are the dominant types for regions 1 and 2, respectively, composites for all EH dates in region 1 and all PH dates for region 2 were created in a fashion similar to that above (i.e., using 3-hourly NARR files to compute MSLP, potential temperature, and 925-hPa winds) for the day of events, as well as $t + 24$ and $t + 48$ h. For region 1, an EH event remains in place through $t + 48$ h (not shown). This may allude to the fact that blocking patterns are important for region 1. For region 2, there is a natural progression for PH to evolve into a BH at $t + 48$ h (not shown). It is therefore possible for a PH to precondition the boundary layer to wildfires more favorable in BH types, especially during the start of BH period before the southerly flow can advect sufficient moist air into the region.

Figure 16 shows a box-and-whiskers plot of the 2-m RH and 925-hPa wind speed for all fire dates areal averaged in both regions 1 and 2 for $t = 0$. The mean RH for regions 1 and 2 is 60%–63% (Fig. 16a), and the average wind speed is ~5.5 m s^{-1} for region 1 and 6.3 m s^{-1} for region 2 (Fig. 16b). Both regions have the same minimum RH (~43%), but the fires in region 2 occur when the RH maximum is higher (maximum RH ~89%) than in region 1 (maximum RH ~74%). Areal average wind speed minimum and maximum values are

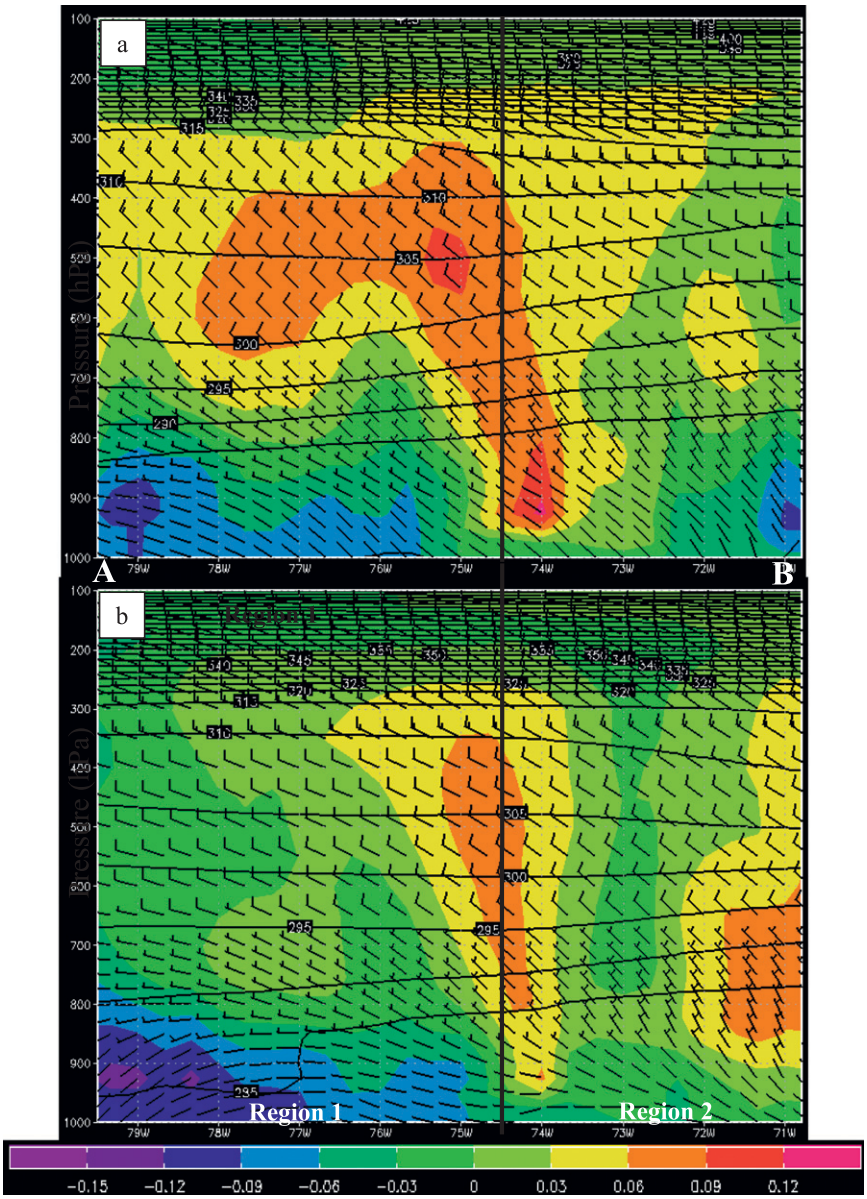

FIG. 10. Composite cross section along 41.5°N over the NEUS (AB in Fig. 9b) at (a) 48 h prior to and (b) the day of ($t = 0$) the region 1 wildfire events showing potential temperature (solid, every 5 K), vertical velocity (color shaded, every 5 Pa s^{-1}), and wind barbs (full barb = 10 m s^{-1}). The thick vertical black line separates regions 1 and 2.

similar for regions 1 and 2. The standard deviations for wind speed are also similar for both regions (3.0 m s^{-1} in region 1 and 2.8 m s^{-1} in region 2).

d. Trajectory analysis

To determine the origin of the large-scale subsidence and associated dry air for regions 1 and 2, trajectories were launched at 2100 UTC starting at 1500 m above ground level (AGL) and integrated backward 48 h using the 3-hourly NARR analyses. A 1500-m starting height was chosen, since the air near the top of the PBL can be mixed down to the surface during the day. This is also high enough to be less influenced by the NARR moist bias previously mentioned in the PBL. Since the PH, EH, and BH synoptic types are most commonly observed, trajectories were generated for actual fire days exhibiting each of these patterns. A mean trajectory was calculated at each of the four points in Fig. 1 by averaging the height and RH of all trajectories launched for a particular synoptic type for both regions 1 and 2.

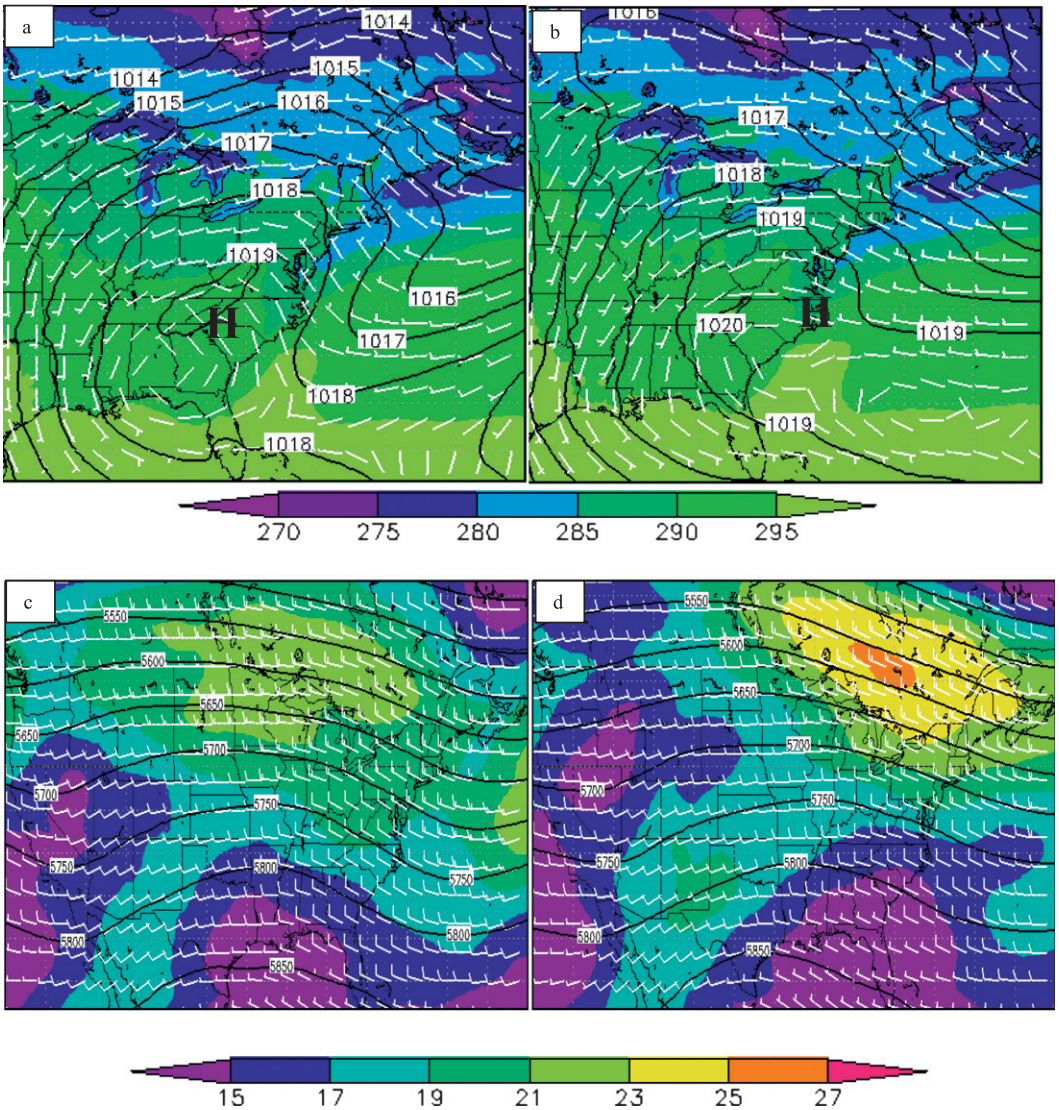

FIG. 11. As in Fig. 7, but for region 2.

Figure 17a shows the average trajectories (A, B, C, and D) for the 28 PH events. Figure 1 shows the origin of the four trajectories, which suggests that the air at $t = 0$ originated over southern Canada at $t - 48$ h. The starting points for two of the four trajectories (B and C) are between 3100 and 3500 m AGL 48 h prior to the fire, while trajectory A begins between 2700 and 3100 m AGL and trajectory D starts between 1900 and 2300 m AGL. This corresponds to 500–2000 m of descent during the 48-h period with northwesterly flow. The RHs start out between 45% and 60% at $t - 48$ h, and the largest decrease in RH occurs for trajectories A and C, which end at ~35%. Trajectory D shows the smallest decrease in RH (~12%).

Figure 17b shows the average of the 32 EH trajectories for points A, B, C, and D. All trajectories originate to the north of the Great Lakes with heights ranging from 2250 to 2750 m. The trajectories curve anticyclonically as they descend to 1500 m over the NEUS. Trajectory B shows the largest subsidence (~2750 m down to 1500 m), while trajectory D has the smallest (~2350 to 1500 m). Trajectory D is at a higher elevation than the other points (~762 m), which could explain why the net downward displacement is less for this trajectory. The RHs start out between 38% and 49% and ends between 35% and 42%. While the PH trajectories exhibit a steady decrease in RH throughout much of the individual trajectories, the EH trajectories show an increase in RH about halfway through the trajectory before decreasing again during the last 24 h of the trajectory.

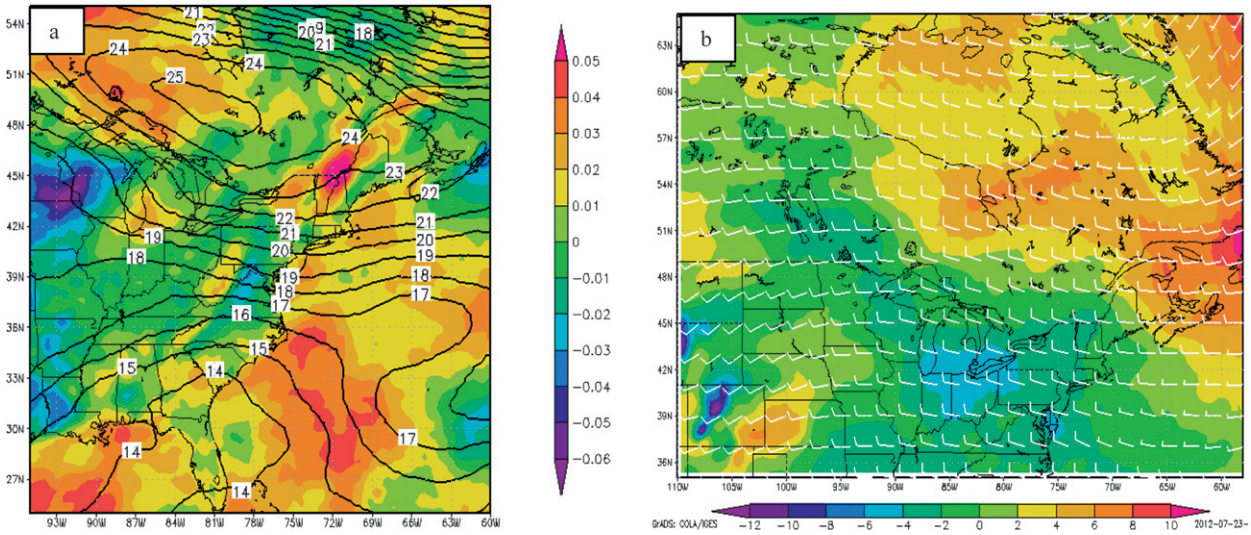

FIG. 12. As in Fig. 8, but for region 2.

For the 24 BH trajectories (Fig. 17c), the trajectories originate over the midwestern United States between 1750 and 2250 m at $t - 48$ h. All but one trajectory (A) fall below 1500 m and then rise to 1500 m at $t = 0$, which suggests that some ascent on the day of the fire is a feature for this synoptic type. The BH type shows little change in RH from the beginning to the end of the trajectories. Trajectories begin and end between 40% and 50%, with some minor increases before the end of the trajectories.

PH events are the dominant synoptic type for region 2 wildfires. The trajectories illustrate greater subsidence associated with these PH events than the EH trajectories in region 1. Trajectory A, which occurs in region 1, spends some time over the coastal waters, which would lead to an increase in RH before arriving at its end point.

e. *Actual wildfire days versus threat days*

One goal of this study was to develop an annual and monthly climatology for actual wildfire days over the NEUS. However, a climatology of actual wildfire days does not necessarily include all days with an elevated wildfire threat, which are days exhibiting elevated potential for the ignition and spread of wildfires. The

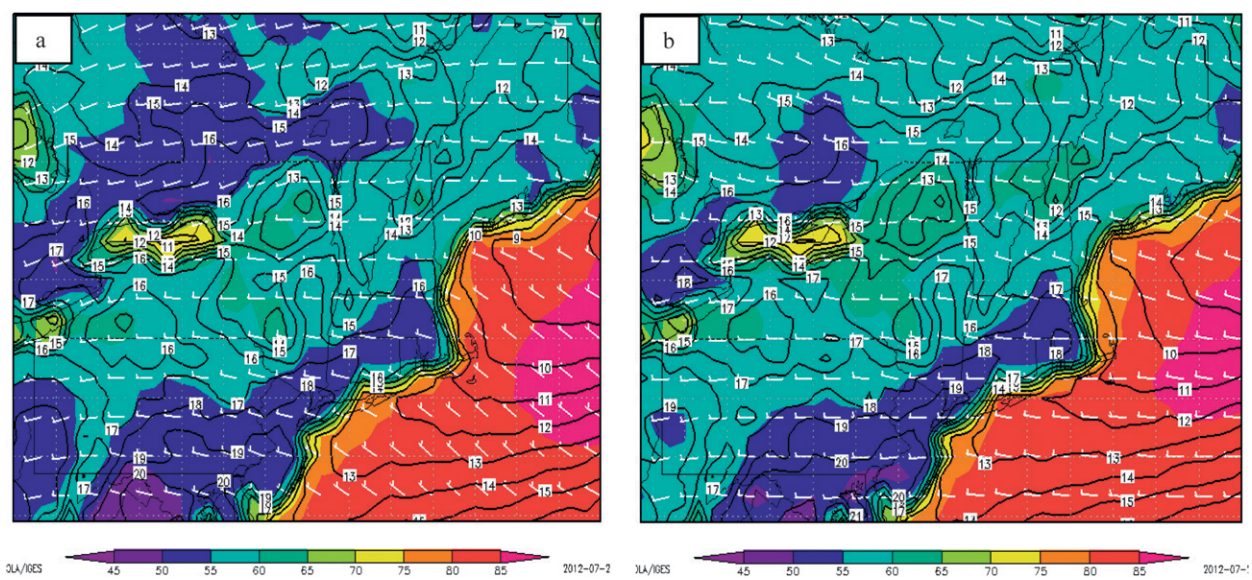

FIG. 13. As in Fig. 9, but for region 2.

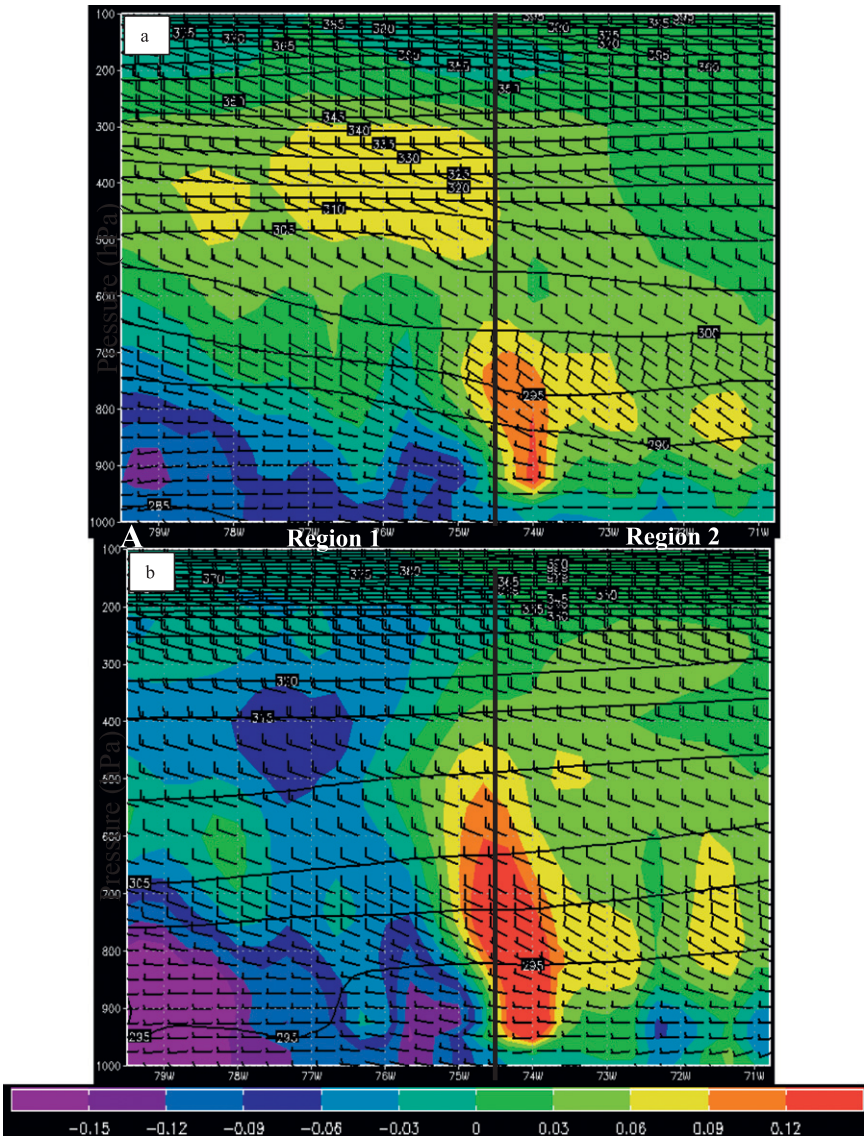

FIG. 14. As in Fig. 10, but for region 2.

meteorological conditions contributing to wildfire threat in the NEUS need to be better understood (Charney et al. 2003; Charney and Fusina 2006; Charney and Keyser 2010). Therefore, in this section an abbreviated analysis of wildfire threat days is presented and compared with the analysis of actual wildfire days.

Building a climatology based upon RFWs in the NEUS is difficult due to their scarcity. However, days of high wildfire threat, which are defined as days on which NFDRS ratings indicate elevated potential for the ignition and spread of wildfires, are more common. Therefore, this climatology was created using days when 50% or greater of the NEUS had a NFDRS rating of "high" or greater according to the Wildland Fire Assessment System (WFAS) database (www.wfas.net). Between January 1999 and December 2009, 194 days were identified that met this criterion. Since WFAS-archived NFDRS maps are only available for entire states, it was not possible to subdivide the events into the two regions shown in Fig. 1.

For the annual wildfire threat climatology (Fig. 18a), the largest peak occurs in 1999, with a secondary peak in 2006. This distribution of wildfire threat days generally corresponds with the actual wildfire day results (Fig. 3). Also, 2007 was one of the least active wildfire threat years (~2.1% of the wildfire threat days occurred in 2007), and it was the least active major wildfire year for region 2 (~2.4%). Anomalously wet and cool meteorological

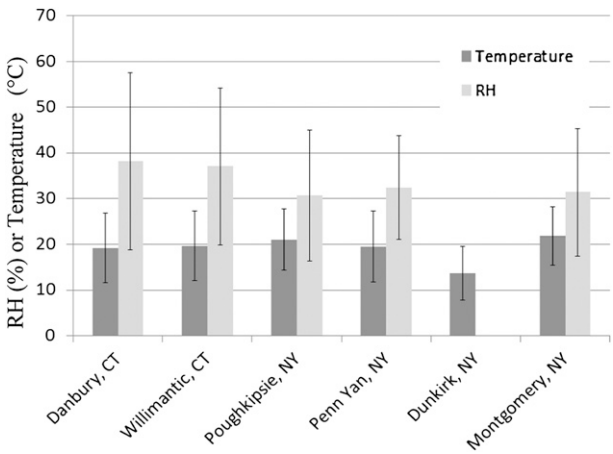

FIG. 15. Average temperature (°C) and RH (%) at 2100 UTC for Danbury (DXR), CT; Willimantic, CT (IJD); Poughkeepsie, NY (POU); Penn Yan, NY (PEO); Dunkirk, NY (DKK); and Montgomery, NY (MGJ), for the fire events in regions 1 and 2. The vertical line represents the first standard deviation. The locations of the stations are shown in Fig. 1.

conditions in April 2007, which was the 3rd wettest and 25th coldest April on record for the NEUS (NOAA 2010), most likely contributed to the small number of actual wildfire and wildfire threat days.

The monthly climatology of wildfire threat (Fig. 18b) documents an increase in the number of wildfire threat days from January (~6%) to February (~13%). This result differs from the climatology of actual fires, where the most substantial increase in actual wildfire days occurs from March to April (Fig. 4). A possible explanation for the discrepancy is that NFDRS does not produce fire danger ratings when there is snow on the ground. In February and March, this practice can produce a large north–south gradient in NFDRS indices as snow in the southern portion of the NEUS melts while the northern sections remain snow covered. Since our criterion requires that 50% of the region exhibit ''high'' or greater fire danger, wildfire threat days become more likely to occur starting in February. Over 30% of the days in February and March exhibited this type of north–south variation, since NFDRS indices were not calculated for 100% of days in the northern NEUS. The number of actual wildfire days does not increase in this time period because humans are the leading cause of wildfire ignitions in the NEUS, and human outdoor activity does not tend to increase until April, when temperatures start to rise.

4. Conclusions

The goal of this study was to develop an annual and monthly climatology for northeast United States (NEUS) wildfires and the associated synoptic weather conditions. The annual and monthly climatology of wildfire events was summed over the NEUS for major wildfire events (>100 acres) and analyzed for two regions: the interior northeast (region 1) and the coastal plain (region 2). There was a peak in wildfire days in 1999 for region 2 and in 2006 for region 1, which corresponded to years of

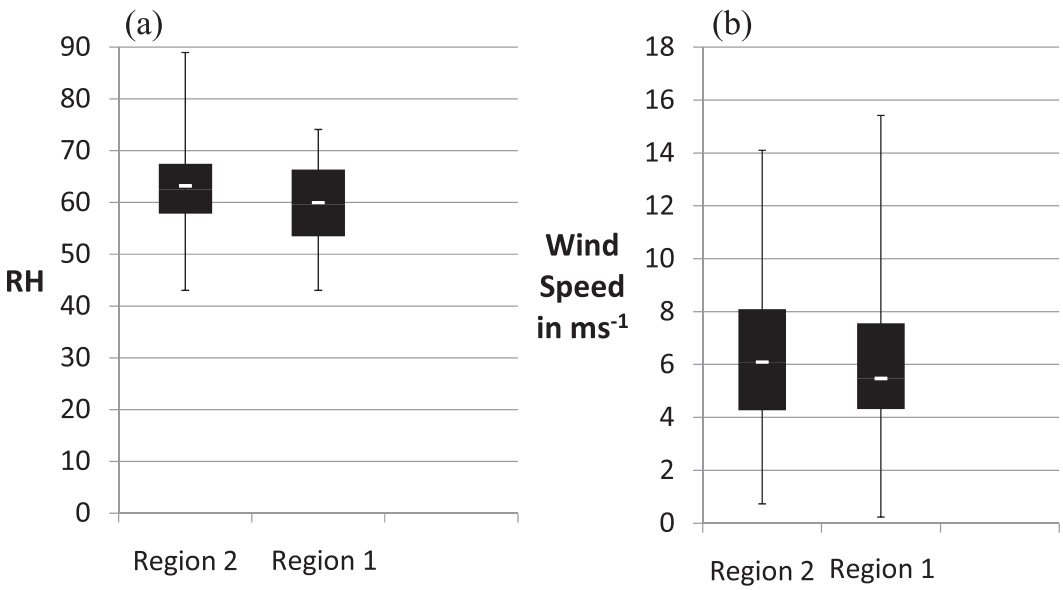

FIG. 16. Box-and-whiskers plot for (a) 2-m RH (%) and (b) 925-hPa wind speed (m s^{-1}) for all wildfires in regions 1 and 2 for t = 0. The mean is given by the thin horizontal white line, the one standard deviation range around the mean is shaded black, and the range of values from the maximum and minimum is given by the thin solid lines.

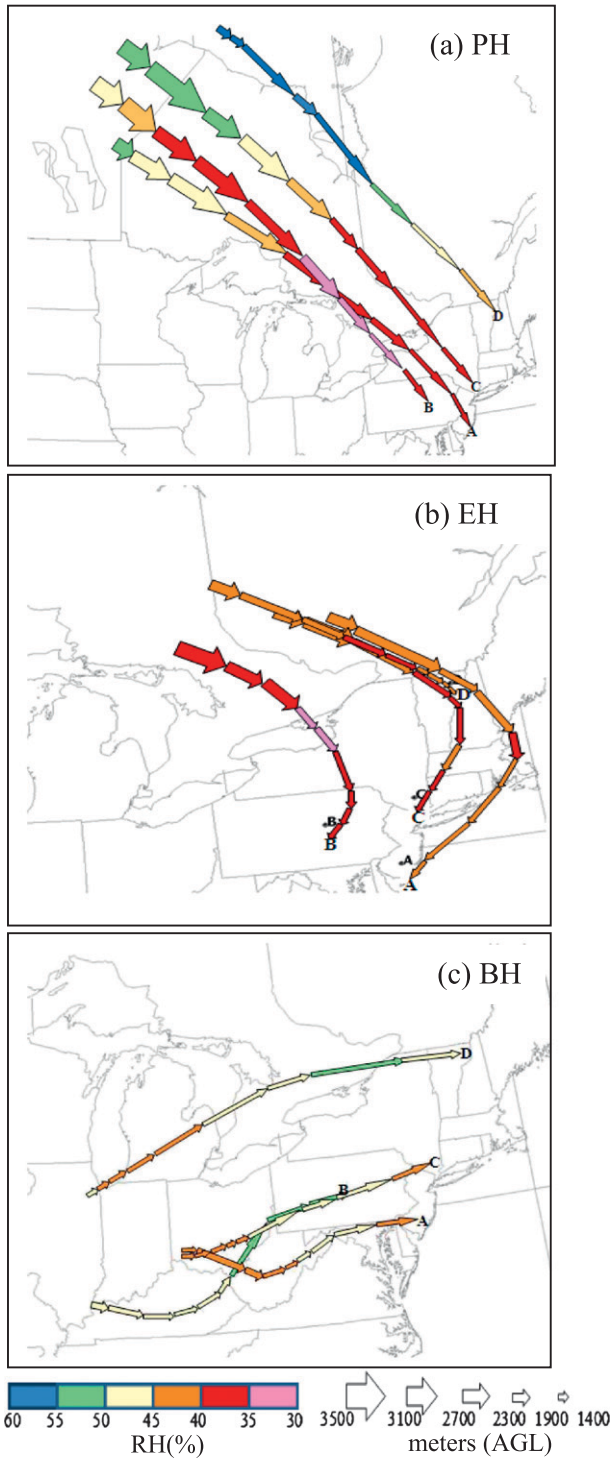

FIG. 17. Average backward trajectory evolution starting at points A–D for all wildfire (a) PH, (b) EH, and (c) BH synoptic types from regions 1 and 2 showing the trajectory height above ground level (arrow thickness in m) and RH (shaded, every 5%). The backward trajectory in 6-h increments, with the ending point 48 h prior to the fire event. The length of the arrow is proportional to the trajectory speed.

anomalously warm and dry conditions. The peak wildfire season over the NEUS is April and May, with the largest number of major wildfires occurring in April. This is likely due to the pre-green-up (leaf out) period across the NEUS, increasing solar radiation, and the continental high pressure systems that commonly move into the region during this time of year. There is a minimum in wildfire activity in the climatological winter (DJF) due to the cool and damp conditions present during this time of year and the presence of snowpack.

The prehigh (PH), extended high (EH), and back of high (BH) surface pressure patterns are the three most common types associated with NEUS wildfire events. The PH is associated with large-scale descent, and the low-level northwesterlies across the NEUS favors downslope flow in the lee of the Appalachians, especially across region 2, where the PH type is most frequent. The EH pattern is the most common type for region 1. This type is associated with an unusually large area of high pressure that slowly moves across the NEUS, thus allowing for persistent dry conditions, which permit the fuels to dry. Southwesterly flow is normally established during the BH synoptic type, with the westerly component allowing for some downslope flow and the southerly component advecting relatively warm air into the NEUS.

Spatial composites using the North American Regional Reanalysis (NARR) show that for region 1 the origination of the high pressure system 2 days before the event is over the eastern Great Lakes region. Over the next 48 h this high pressure becomes centered over NEUS to yield an EH pressure pattern. For region 2, a PH type is already in place over the NEUS 2 days before the event, and it is nearly stationary over the 48-h period. The RH is smaller and the 925-hPa wind speeds are similar over region 1 for $t - 48$ h and $t = 0$, while there is little change in RH in region 2. A comparison between NARR and six surface observations in the NEUS shows that the NARR was too moist by up to 25%, and thus the RH composites do not represent the proper amplitude of the drying associated with these events. The observations have RH values of 30%–40% during the late afternoon for these fire events. The observed RH is still higher than the RFW criterion of <30%. This suggests that the RFW RH criterion may be too low for the NEUS, and a <40% threshold may be more appropriate.

HYSPLIT back trajectories were completed starting at 1500 m (~850 hPa). The air originating at the 850-hPa level is important, since daytime heating allows for convective mixing, and thus some of this dry air can be transported to the surface. The PH synoptic type undergoes the most subsidence and largest decrease in RH for trajectories originating at midlevels over south-central

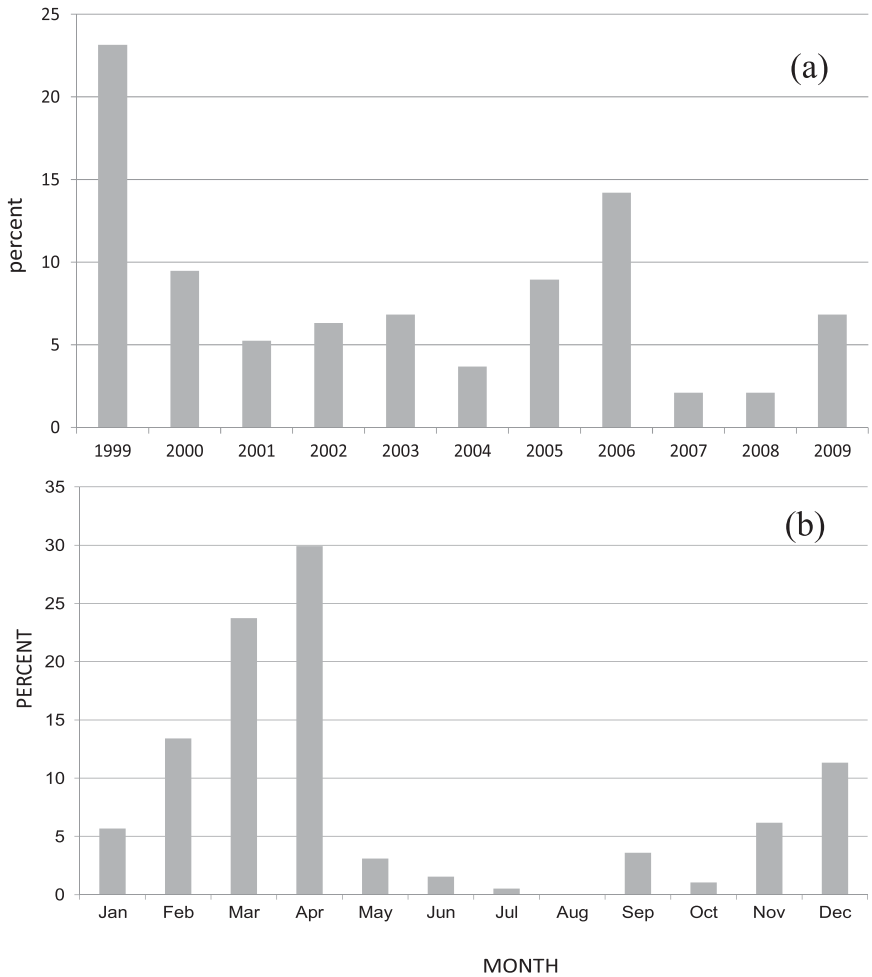

FIG. 18. (a) Annual and (b) monthly wildfire threat climatology (%) for the entire NEUS between 1999 and 2009.

Canada. In contrast, the BH trajectories experience the least subsidence and decrease in RH on average. Approximately 29% of all BH events showed some origin over the Rockies up to 120 h prior to the events. The trajectory changes for subsidence and RH for the EH type are between the PH and BH synoptic types.

Wildfires are not common to the NEUS, and thus the sample size was limited. However, the most common pressure pattern to effect region 2 (EH) was found to be statistically significant. Meanwhile, in region 2, PH, EH, and BH were statistically significant compared to the other types. Since the large-scale composite evolution for the two regions is similar to the dominant Yarnal pressure patterns for each region, the composites are also likely providing useful information relative to climatology. The dry 15%–25% RH anomalies at the surface were also found to be significant relative to climatology.

The results from this study are useful in an operational forecast setting. For example, noting that a PH- or EH-type synoptic pattern will develop over the NEUS after a period of dry weather would be a signal to forecasters that conditions may be favorable for wildfires to occur. In contrast, an EL, CF, HN, or ST pattern will allow forecasters to realize that wildfires are less likely to occur. For the seasonal climatology of wildfire threat and actual wildfire days, a forecaster will be better prepared to recognize conditions during the peak of wildfire season of April–May, while still noting that wildfires are possible for other months.

Criteria for RFWs are determined by the NWS along with representatives from the fire management community (T. Morrin, NWS-NYC, 2011, personal communication). However, these criteria are not established based upon an analysis of the climatological frequency of high wildfire danger days and actual wildfire days.

Our analysis suggests that RFWs (and FWWs) may not capture an optimal percentage of high wildfire days or actual wildfire days. This study could be used to help reevaluate the criteria for RFWs and FWWs. Finally, the information in this study may also be used to differentiate between unusual wildfire weather events and those that are more routine.

Acknowledgments. This work was supported by a research joint venture agreement between Stony Brook University and the U.S. Forest Service (08-JV-11242306-093). We thank the three anonymous reviewers for their comments and suggestions.

REFERENCES

Bluestein, H. B., 1992: *Principles of Kinematics and Dynamics.* Vol. 1, *Synoptic-Dynamic Meteorology in Midlatitudes,* Oxford University Press, 431 pp.

Buckley, C., 2008: Forest fire scorches 3,000 acres in Ulster Park. *New York Times,* 21 April. [Available online at http://www.nytimes.com/2008/04/21/nyregion/21minnewaska.html?ref=nyregion.]

Bureau of Meteorology, cited 2009: Bushfire weather. [Available online at http://www.bom.gov.au/weather-services/bushfire/about-bushfire-weather.shtml.]

Burgan, R. E., 1988: 1988 revisions to the 1978 National Fire-Danger Rating System. USDA Forest Service Research Paper SE-273, Southeastern Forest Experiment Station, Asheville, NC, 39 pp [Available online at http://www.srs.fs.usda.gov/pubs/rp/rp_se273.pdf.]

Charney, J. J., and L. A. Fusina, 2006: Employing numerical weather models to enhance fire weather and fire behavior predictions. *Fuels Management—How to Measure Success:* Portland, OR, International Association of Wildland Fire, RMRS-P-41, 769–786.

——, and D. Keyser, 2010: Mesoscale model simulation of the meteorological conditions during the 2 June 2002 Double Trouble State Park wildfire. *Int. J. Wildland Fire,* **19,** 427–448.

——, X. Bian, B. E. Potter, and W. E. Heilman, 2003: The role of a stratospheric intrusion in the evolution of the Double Trouble State Park wildfire. Preprints, *Fifth Symp. on Fire and Forest Meteorology,* Orlando, FL, Amer. Meteor. Soc., P5.3. [Available online at http://ams.confex.com/ams/pdfpapers/65830.pdf.]

Draxler, R. R., and G. D. Rolph, cited 2012: HYSPLIT—Hybrid Single-Particle Lagrangian Integrated Trajectory model. NOAA/ARL. [Available online at http://ready.arl.noaa.gov/HYSPLIT.php.]

Hamilton, C., and I. Ostapow, 2009: Long Island, NY—Central Pine Barrens. National Database of State and Local Wildfire Hazard Mitigation Programs, USDA Forest Service. [Available online at http://www.wildfireprograms.com/search.html?search=advanced&string=SUNRISE%20FIRE&state=&displayId=283.]

Kaplan, M. L., C. Huang, Y. L. Lin, and J. J. Charney, 2008: The development of extremely dry surface air due to vertical exchanges under the exit region of a jet streak. *Meteor. Atmos. Phys.,* **102,** 63–85.

Kassomenos, P. 2010: Synoptic circulation control on wild fire occurrence. *Phys. Chem. Earth,* **35A/B/C,** 544–552.

Keetch, J. J., and G. M. Byram, 1968: A drought index for forest fire control. USDA Forest Service Research Paper SE-38, Southeastern Forest Experiment Station, Asheville, NC, 35 pp.

Mesinger, F., and Coauthors, 2006: A long-term, consistent, high-resolution climate dataset for the North American domain, as a major improvement upon the earlier global reanalysis datasets in both resolution and accuracy. *Bull. Amer. Meteor. Soc.,* **87,** 343–360.

NIFC, 2008: Fire information—Wildland fire statistics. National Interagency Fire Center. [Available online at http://www.nifc.gov/fireInfo/fireInfo_stats_YTD2008.html.]

NOAA, cited 2010: State of the climate. National Climatic Data Center, Asheville, NC. [Available online at http://www.ncdc.noaa.gov/sotc/.]

——, cited 2011: Plot time series. National Climatic Data Center, Asheville, NC. [Available online at http://www.ncdc.noaa.gov/temp-and-precip/time-series/.]

Northeast States Emergency Consortium, cited 2012: Fires. [Available online at http://www.nesec.org/hazards/fires.cfm.]

Novak, D. R., and B. A. Colle, 2006: Observations of multiple sea breeze boundaries during an unseasonably warm day in metropolitan New York City. *Bull. Amer. Meteor. Soc.,* **87,** 169–174.

NWS, 2008: Fire weather ready reference. Station duty manual. Vol. 2., 75 pp. [Available from WFO—New York, Bldg. NWS-1, 174 Brookhaven Ave., Upton, NY 11973.]

Rolph, G. D., 2012: READY—Real-time Environmental Applications and Display System. NOAA Air Resources Laboratory. [Available online at http://ready.arl.noaa.gov.]

Rorig, M. L., and S. A. Ferguson, 2002: The 2000 fire season: Lightning-caused fires. *J. Appl. Meteor.,* **41,** 786–791.

Rothermel, R. C., 1983: How to predict the spread rate and intensity of forest and range fires. Intermountain Research Station General Tech. Rep. INT-143, USDA Forest Service, Ogden, UT, 161 pp.

Schaefer, V. J., 1957: The relationship of jet streams to forest wildfires. *J. For.,* **55,** 419–425.

Schroeder, M. J., M. Glovinsky M., V. F. Henricks, F. C. Hood, and M. K. Hull, 1964: Synoptic weather types associated with critical fire weather. Defense Documentation Center for Scientific and Technical Information, Cameron Station Alexandria, VA, 492 pp.

Takle, E. S., D. J. Bramer, W. E. Hellman, and M. R. Thompson, 1994: A synoptic climatology for forest fires in the NEUS and future implications from GCM simulations. *Int. J. Wildland Fire,* **4,** 217–224.

Trenberth, K. E., 1978: On the interpretation of the diagnostic quasi-geostrophic omega equation. *Mon. Wea. Rev.,* **106,** 131–137.

Viney, N. R., 1991: A review of fine fuel moisture modeling. *Int. J. Wildland Fire,* **1,** 215–234.

Yarnal, B., 1993: *Synoptic Climatology in Environmental Analysis: A Primer*. Belhaven Press, 256 pp.

Zwiers, F. W., 1990: The effect of serial correlation on statistical inferences made with resampling procedures. *J. Climate,* **3,** 1452–1460.